Unique inhibitory synapse with particularly rich endocannabinoid signaling machinery on pyramidal neurons in basal amygdaloid nucleus

Takayuki Yoshida[a,b,c], Motokazu Uchigashima[a], Miwako Yamasaki[a], Istvan Katona[d], Maya Yamazaki[e], Kenji Sakimura[e,f], Masanobu Kano[c,g], Mitsuhiro Yoshioka[b], and Masahiko Watanabe[a,f,1]

Departments of [a]Anatomy and [b]Neuropharmacology, Hokkaido University Graduate School of Medicine, Sapporo 060-8638, Japan; [c]Department of Cellular Neuroscience, Graduate School of Medical Science, Osaka University, Suita 565-0871, Japan; [d]Institute of Experimental Medicine, Hungarian Academy of Sciences, Szigony utca 43, 1083, Budapest, Hungary; [e]Department of Cellular Neurobiology, Brain Research Institute, Niigata University, Niigata 951-8585, Japan; [f]Japan Science and Technology Agency, Core Research for Evolutional Science and Technology, Sanbocho, Tokyo 102-0075, Japan; and [g]Department of Neurophysiology, Graduate School of Medicine, University of Tokyo, Tokyo 113-0033, Japan

Edited* by Tomas G. M. Hökfelt, Karolinska Institutet, Stockholm, Sweden, and approved January 12, 2011 (received for review September 2, 2010)

2-Arachidonoylglycerol (2-AG) is the endocannabinoid that mediates retrograde suppression of synaptic transmission in the brain. 2-AG is synthesized in activated postsynaptic neurons by *sn*-1-specific diacylglycerol lipase (DGL), binds to presynaptic cannabinoid CB_1 receptors, suppresses neurotransmitter release, and is degraded mainly by monoacylglycerol lipase (MGL). In the basolateral amygdala complex, it has been demonstrated that CB_1 is particularly enriched in axon terminals of cholecystokinin (CCK)-positive GABAergic interneurons, induces short- and long-term depression at inhibitory synapses, and is involved in extinction of fear memory. Here, we clarified a unique molecular convergence of DGLα, CB_1, and MGL at specific inhibitory synapses in the basal nucleus (BA), but not lateral nucleus, of the basolateral amygdala. The synapses, termed invaginating synapses, consisted of conventional symmetrical contact and unique perisynaptic invagination of nerve terminals into perikarya. At invaginating synapses, DGLα was preferentially recruited to concave somatic membrane of postsynaptic pyramidal neurons, whereas invaginating presynaptic terminals highly expressed CB_1, MGL, and CCK. No such molecular convergence was seen for flat perisomatic synapses made by parvalbumin-positive interneurons. On the other hand, DGLα and CB_1 were expressed weakly at axospinous excitatory synapses. Consistent with these morphological data, thresholds for DGLα-mediated depolarization-induced retrograde suppression were much lower for inhibitory synapses than for excitatory synapses in BA pyramidal neurons. Moreover, depolarization-induced suppression was readily saturated for inhibition, but never for excitation. These findings suggest that perisomatic inhibition by invaginating synapses is a key target of 2-AG-mediated control of the excitability of BA pyramidal neurons.

retrograde signaling | metabotropic glutamate receptor | muscarinic acetylcholine receptor | depolarization-induced suppression of inhibition | depolarization-induced suppression of excitation

Marijuana and other derivatives of the plant *Cannabis sativa* exert diverse neuropsychopharmacological actions, such as hallucination, euphoria, sedation, memory impairment, anxiolytic effect, appetite stimulation, motor deficit, and pain relief. These actions are mediated by Δ9-tetrahydrocannabinol (Δ9-THC), an active component of cannabis, through its binding to cannabinoid CB_1 receptors (1). CB_1 is particularly abundant in specific types of neurons, is selective to presynaptic elements, and induces short- and long-term forms of retrograde suppression of neurotransmitter release (1). In the brain, 2-arachidonoylglycerol (2-AG) is the major endogenous cannabinoid, synthesized in postsynaptic neurons by *sn*-1-specific diacylglycerol lipase (DGL) (2), and degraded mainly by monoacylglycerol lipase (MGL) (3, 4). 2-AG synthesis is facilitated when depolarization of postsynaptic neurons is combined with $G_{q/11}$-coupled receptor activation (1). Selective postsynaptic expression of DGLα at around dendritic spines and its colocalization with $G_{q/11}$-coupled receptors provide given neurons with the molecular basis and further the strategy to balance the excitation and inhibition according to synaptic organization and internal state of the brain (1, 5–8).

The amygdala plays critical roles in associative processes of aversive emotions (9), and intake of cannabinoids elicits dose-dependent and biphasic effects on emotionality (10, 11). Of several anatomically and functionally distinct nuclei, CB_1 is particularly abundant in the basolateral amygdala complex (BLA) (12–16) and modulates the consolidation of memories for emotionally arousing experiences (17, 18). In the BLA, CB_1 is enriched in axon terminals of cholecystokinin (CCK)-positive interneurons, regulates transmission (19) and long-term depression at inhibitory synapses, and is involved in extinction of aversive memories (20–22).

In this study, we report that DGLα, CB_1, and MGL intensively accumulate at the invaginating type of perisomatic inhibitory synapses in the basal nucleus (BA), but not lateral nucleus (LA), of the BLA. This unique synapse was formed by CCK-positive interneuron terminals on pyramidal neurons, whereas no such accumulation was seen for the flat type of perisomatic inhibitory synapses made by parvalbumin-positive interneurons. In BA pyramidal neurons, depolarization-induced suppression of inhibition (DSI) was robustly induced with short depolarizing pulses and readily saturated with longer pulses, whereas depolarization-induced suppression of excitation (DSE) required longer depolarization for induction and was never saturated. Our findings suggest that 2-AG signaling molecules are preferentially allocated to invaginating synapses to effectively shut off the perisomatic inhibition to BA pyramidal neurons.

Results

DGLα Is Clustered at Invaginating Synapse on BA Pyramidal Neuron. In the amygdala of adult C57BL/6 mice, cellular expression of DGLα was determined by fluorescent in situ hybridization (FISH) by using fluorescein- or digoxigenin-labeled riboprobes. Characteristic cellular labeling for DGLα mRNA was yielded with use of antisense riboprobe (Fig. S1*A*), but not sense probe (Fig. S1*B*), in various amygdala nuclei, including the BA, LA, central nucleus, and medial and lateral intercalated cell masses (Fig. S1*C*). Of these nuclei, relatively high levels were noted in the BA and LA; they were identified by cortex-like neuronal composition, i.e., many pyramidal neurons expressing type-1 vesicular glutamate transporter (VGluT1) mRNA (Fig. S1*D*) with a few interneurons

Author contributions: T.Y., M.K., M. Yoshioka, and M.W. designed research; T.Y., M.U., and M. Yamasaki performed research; I.K., M. Yamazaki, and K.S. contributed new reagents/analytic tools; T.Y., M.U., and M. Yamasaki analyzed data; and T.Y., M.K., and M.W. wrote the paper.

The authors declare no conflict of interest.

*This Direct Submission article had a prearranged editor.

[1]To whom correspondence should be addressed. E-mail: watamasa@med.hokudai.ac.jp.

This article contains supporting information online at www.pnas.org/lookup/suppl/doi:10.1073/pnas.1012875108/-/DCSupplemental.

expressing 67-kDa glutamic acid decarboxylase (GAD67) mRNA (Fig. S1*E*). In the BA, double FISH demonstrated that DGLα mRNA was highly expressed in VGluT1 mRNA-expressing pyramidal neurons (Fig. 1*A*), whereas it was considerably low in GAD67 mRNA-expressing interneurons (Fig. 1*B*).

DGLα immunolabeling was detected in the amygdala (Fig. 1 *C–E*), and the specificity was verified by blank labeling in DGLα-knockout mice (Fig. 1*D, Inset*). At high magnifications, fine punctate immunolabeling in the neuropil was common to the BA and LA (Fig. 1 *F* and *G*). These neuropil puncta were often distributed around Ca^{2+}/calmodulin-dependent kinase IIα (CaMKIIα)-positive dendrites (Fig. 1*H*), i.e., dendrites of pyramidal neurons. Coarse perisomatic clusters of DGLα were found in the BA (Fig. 1*F*, arrowheads), but not in other amygdala nuclei including the LA (Fig. 1*G* and Fig. S2). Intriguingly, these perisomatic puncta were confronted with GAD-positive terminals (Fig. 1*H*, arrowheads) and found on the soma of CaMKIIα-positive pyramidal neurons, but not GAD-positive interneurons, suggesting unique perisomatic accumulation of DGLα at inhibitory synapses on BA pyramidal neurons.

Ultrastructural localization of DGLα was examined by preembedding silver-enhanced immunogold electron microscopy (Fig. 2 *A–E*). In the soma of BA pyramidal neurons, metal particles were mostly attached to the cell membrane with a few being dispersed intracellularly around vesicles and endoplasmic reticulum (Fig. 2*A*). Of note, metal particles were clustered on concave or ruffled somatic membrane, to which nerve terminals protruded or invaginated (Fig. 2 *A* and *B*, arrows). Next to the invagination, invaginating nerve terminals formed symmetrical synaptic contact (Fig. 2 *A* and *B*, open arrowheads). We also found another type of perisomatic synapses, which showed neither specific DGLα accumulation nor invagination (Fig. 2*A*). For descriptive convenience, we termed the two perisomatic synapses

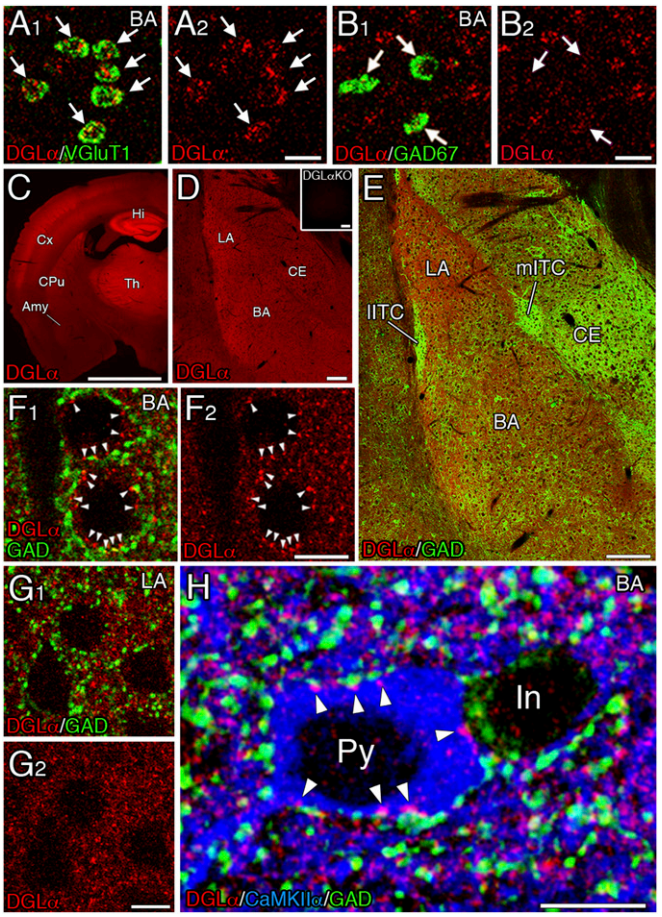

Fig. 1. Abundant expression and perisomatic clustering of DGLα in pyramidal neurons of the basal nucleus of the amygdala. (*A* and *B*) Double FISH showing higher expression of DGLα mRNA (red) in pyramidal neurons expressing VGluT1 mRNA (*A*, green) than in interneurons expressing GAD67 mRNA (*B*, green) in the BA. (*C* and *D*) Single immunofluorescence for DGLα in the forebrain (*C*) and amygdala (*D*). Specificity of DGLα immunolabeling is verified by blank labeling in DGLα-knockout mice (*D Inset*). (*E–G*) Double immunofluorescence for DGLα (red) and GAD (green). Coarse perisomatic clusters of DGLα are detected in the BA (*F*, arrowheads), but not in the lateral nucleus (LA; *G*). (*H*) Triple immunofluorescence for DGLα (red), GAD (green), and CaMKIIα (blue) in the BA. Perisomatic DGLα clusters are preferentially observed in CaMKIIα-positive pyramidal neurons (Py), but not in CaMKIIα-negative/GAD-positive inhibitory interneurons (In). Amy, amygdala; CE, central nucleus, CPu, caudate-putamen; Cx, cerebral cortex; Hi, hippocampus; mITC/lITC, medial and lateral intercalated cell masses, Th, thalamus. (Scale bars: *A* and *B*, 20 μm; C, 1 mm; *D* and *E*, 200 μm; *F–H*, 10 μm.)

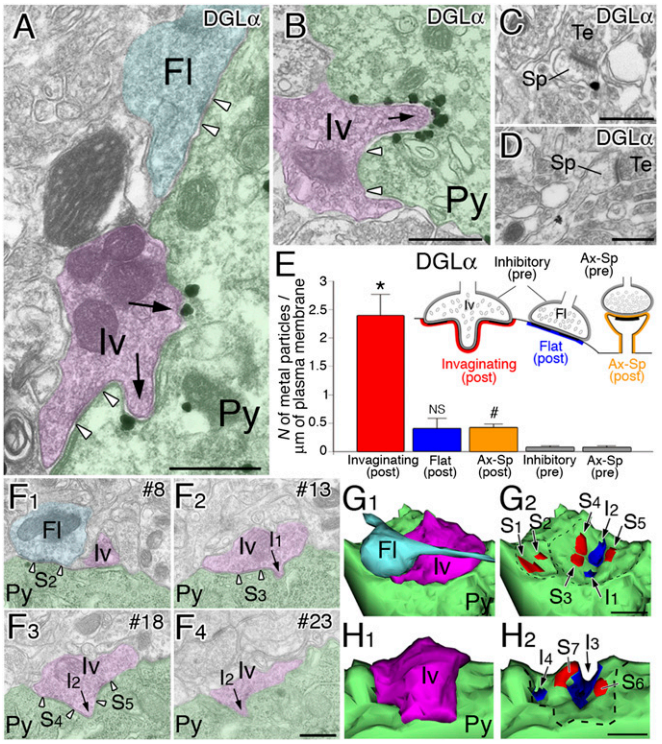

Fig. 2. Silver-enhanced immunogold electron microscopy demonstrating intensive accumulation of DGLα at invaginating synapses on BA pyramidal neurons. (*A* and *B*) DGLα is concentrated on the somatic membrane of pyramidal neurons (Py) that apposes to invaginating terminals (arrows, Iv). However, no particular labeling is seen for terminals forming the flat type of perisomatic synapses (Fl). Open arrowheads indicate the edges of symmetrical synaptic contact. (*C* and *D*) A few metal particles are detected in the head and neck portions of dendritic spines (Sp) forming asymmetrical synapses with putative excitatory terminals (Te). (*E*) Labeling density of metal particles for DGLα in the postsynaptic membrane of invaginating, flat, or axospinous synapses (colored portions for quantitative measurement), and in the presynaptic membrane of inhibitory (symmetrical) or axospinous synapses (gray portions). Using 50 electron micrographs taken from three mice, we analyzed the total number of 19, 18, 200, 35, and 189 synaptic elements. $*P < 0.01$ compared with all other labelings; NS, $P > 0.05$ compared with presynaptic labeling at inhibitory synapses; $\#P < 0.01$ compared with presynaptic labeling at axospinous synapses, Mann–Whitney *U* test. (*F–H*) Serial electron microscopic images (*F*) and 3D reconstruction of invaginating perisomatic synapses (*G* and *H*) in BA pyramidal neurons. *G* was reconstructed from 24 serial sections, including those shown in *F*. Invaginating terminal (Iv), flat terminal (Fl), and pyramidal neuron soma (Py) are pseudocolored in purple, light blue, or green, respectively. Individual sites of invagination (I1–I4) and synaptic contact (S1–S7) are indicated by arrows or open arrowheads, respectively, in *F*, and by blue or red area, respectively, in *G* and *H*. (Scale bars: 500 nm.)

invaginating and flat synapses. In the neuropil, labeling for DGLα was also found on dendritic spines forming asymmetrical synapses, but apparently weak in labeling density compared with invaginating perisomatic synapses (Fig. 2 *C* and *D*). Labeling density was quantified by counting metal particles attaching the cell membrane. The density in the postsynaptic side of invaginating synapses was six times higher than that of flat perisomatic synapses or axospinous synapses, showing significant differences (Fig. 2*E*). Considering that postsynaptic labeling at flat perisomatic synapses or at axospinous synapses was still higher than their presynaptic labeling, DGLα is thus exclusive on the postsynaptic elements of BA pyramidal neurons with intensive accumulation at invaginating synapses.

The morphology of invaginating synapses was investigated by serial electron microscopy (Fig. 2*F*), and two reconstructed cases are shown in Fig. 2 *G* and *H*. While passing by pyramidal neurons, axons formed terminal swellings that made several symmetrical synaptic contacts (Fig. 2*F*, open arrowheads; Fig. 2 *G* and *H*, red portions S1–S7). Between and around the synaptic contacts, nerve terminals made several invaginations on to pyramidal neurons (Fig. 2*F*, arrows; Fig. 2 *G* and *H*, blue portions I1–I4). Thus, invaginating synapses consist of multiple synaptic contacts and invaginations beneath single inhibitory terminals. Therefore, DGLα is highly expressed in BA pyramidal neurons, and preferentially recruited to the cell membrane facing inhibitory invaginating terminals.

Perisomatic DGLα Clusters Selectively Appose to CB_1-Expressing Terminals. Next, we examined cellular expression and subcellular localization of CB_1. Consistent with previous reports (12, 13, 15, 16), CB_1 mRNA was expressed in various amygdala nuclei with the highest level in the BA (Fig. S3 *A* and *B*), where it was high in CCK mRNA-expressing GABAergic interneurons (Fig. S3 *C* and *E*, large arrows), low in VGluT1 mRNA-expressing pyramidal neurons (Fig. S3*D*, small arrows), and negative in parvalbumin mRNA-expressing GABAergic interneurons (Fig. S3 *C* and *F*, arrowheads). The distinct cellular expression was reflected in distinct terminal labeling for CB_1. CB_1 immunofluorescence was much more intense in inhibitory terminals expressing vesicular inhibitory amino acid transporter (VIAAT; Fig. S3*G*) than in excitatory terminals expressing VGluT1 (Fig. S3*H*). Of inhibitory terminals, CB_1 was intense in those expressing CCK (Fig. S3*I*), but negative in those expressing parvalbumin (Fig. S3*J*). The specificity of CB_1 immunohistochemistry was confirmed by blank labeling in CB_1-knockout mice (Fig. S3 *K* and *L*).

Then, we pursued the relationship of perisomatic DGLα clusters to CB_1-positive terminals in BA pyramidal neurons. Immunofluorescence for DGLα (Fig. 3*A*, red) and CB_1 (green) revealed that 94% of perisomatic DGLα clusters (46 of 49 clusters, arrowheads) were apposed to CB_1-positive perisomatic terminals. Only 5% of CB_1-negative/VIAAT-positive perisomatic terminals (6 of 123 terminals) were apposed to perisomatic DGLα clusters (Fig. S4, arrows). Perisomatic localization of DGLα and CB_1 was preserved in mutant mice lacking CB_1 or DGLα, respectively (Fig. S5), indicating that perisomatic targeting of one molecule does not depend on the expression of the other. Such a good apposition was also confirmed for DGLα (Fig, 3*B*, red) and CCK (green).

Heavy immunogold labeling for CB_1 was observed in terminals forming invaginating perisomatic synapses (Fig. 4 *A* and *B*). In contrast, terminals forming flat perisomatic synapses had no significant CB_1 labeling (Fig. 4*B*) but were labeled for parvalbumin (Fig. 4*F*). In the neuropil, low levels of CB_1 were observed on excitatory terminals forming asymmetrical synapse on to dendritic spines (Fig. 4 *C* and *D*). By counting immunoparticles, the density of CB_1 labeling was 8 times higher in terminals forming invaginating perisomatic synapses than in excitatory terminals forming axospinous synapses (Fig. 4*E*). The density in these terminals was significantly higher than that in terminals forming flat synapses and that in postsynaptic membrane of inhibitory and axospinous synapses (Fig. 4*E*). Therefore, high levels of DGLα and CB_1 are preferentially recruited to the post- or presynaptic element, respectively, at invaginating inhibitory synapses on BA pyramidal neurons.

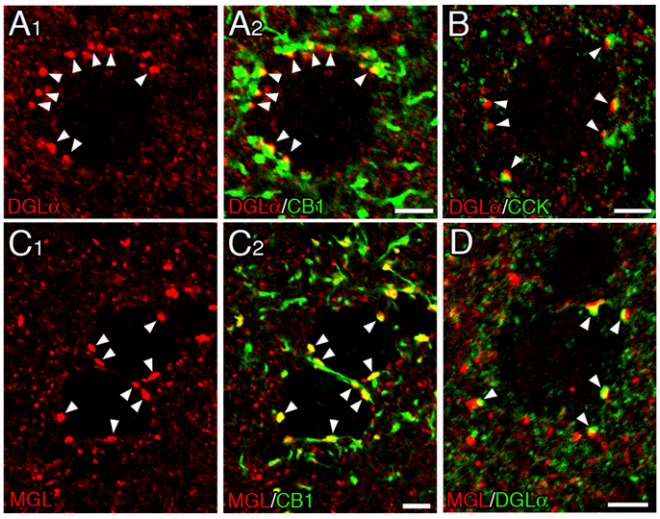

Fig. 3. Perisomatic DGLα clusters are selectively apposed to interneuron terminals expressing CB_1, CCK, and MGL. (*A* and *B*) Immunofluorescence for DGLα (red) and CB_1 (*A*, green) or CCK (*B*, green). Note selective apposition of perisomatic DGLα clusters to CB_1-positive (*A*, arrowhead) or CCK-positive (*B*, arrowhead) terminals. (*C*) MGL (red) is highly expressed in CB_1-positive terminals (green). (*D*) MGL (red) is well apposed to perisomatic DGLα clusters (green). (Scale bars, 5 μm.)

MGL Is Coexpressed with CB_1 and Apposed to DGLα Clusters. We examined immunohistochemical distribution of a major degrading enzyme MGL, whose specificity was confirmed by blank labeling in MGL-knockout mice (Fig. S6). MGL formed intense clusters around BA pyramidal neuron, and overlapped almost completely with CB_1 in perisomatic terminals (Fig, 3*C*). As is the case for CB_1 (Fig. 3*A*), 95% of perisomatic DGLα clusters (62 of 65 clusters, arrowheads) were apposed to MGL-positive perisomatic terminals, whereas 3% of MGL-negative/VIAAT-positive perisomatic terminals (3 of 101 terminals) were apposed to perisomatic DGLα clusters (Fig. 3*D*). Thus, all of the key molecules in the 2-AG–mediated retrograde signaling preferentially accumulate at invaginating synapses in the BA.

DSI Is More Readily Induced and Saturated than DSE in BA Pyramidal Neuron. Inhibitory and excitatory postsynaptic currents (IPSCs and EPSCs) are transiently suppressed after depolarization of postsynaptic neurons through retrograde endocannabinoid signaling; this phenomenon is known as DSI and DSE (23–26). In the BLA, it has been reported that DSI and DSE as well as long-term depression at inhibitory synapses are induced by CB_1 activation (19, 20, 27–29). In the present study, we compared induction profiles of DSI and DSE by recording from BA pyramidal neurons in acute slices (Fig. 5). Pyramidal neurons were identified with fluorescent tracer labeling by morphological characteristics of multipolar dendritic arbors studded with spines (Fig. S7).

Depolarization of BA neurons from −70 mV to 0 mV caused significant reduction of IPSC and EPSC amplitudes, and this reduction was completely blocked by 5 μM of CB_1 antagonist AM251 (DSI magnitude: control, 52.6 ± 2.8%, n = 35 AM251, 94.8 ± 3.0%, n = 7; DSE magnitude: control, 58.7 ± 4.1%, n = 19, AM251, 97.9 ± 2.2%, n = 5) (Fig. 5 *A* and *B*). The paired-pulse ratio (PPR, second PSC/first PSC, interstimulus interval at 50 ms) was increased after depolarization (PPR of IPSC: before, 0.74 ± 0.02, after, 0.84 ± 0.03, n = 42; PPR of EPSC: before, 1.42 ± 0.03, after, 1.66 ± 0.11, n = 19), and this increment was blocked by AM251 (PPR of IPSC: before, 0.75 ± 0.02, after, 0.79 ± 0.05, n = 10; PPR of EPSC: before, 1.49 ± 0.03, after, 1.5 ± 0.07, n = 18) (Fig. 5 *A* and *B*, *Insets*). Application of 5 μM AM251 alone pro-

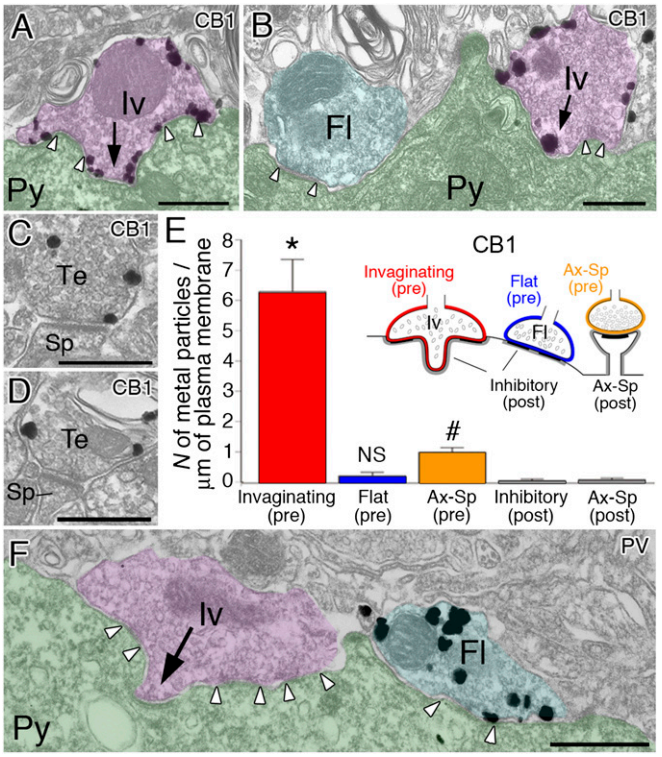

Fig. 4. Silver-enhanced immunogold electron microscopy demonstrating heavy immunoparticle labeling for CB_1 in presynaptic terminals forming invaginating synapses on BA pyramidal neurons. (*A–D*) CB_1 labeling is detected intensely on terminals forming invaginating perisomatic synapses (Iv; *A* and *B*) and weakly on those forming axospinous synapses (*C* and *D*) in pyramidal neurons (Py). No significant labeling is seen for terminals forming flat perisomatic synapses (Fl, *B*). (*E*) Labeling density for CB_1 in the presynaptic membrane of invaginating, flat, or axospinous synapses (colored portions for quantitative measurement) and in the postsynaptic membrane of inhibitory (symmetrical) or axospinous synapses (gray portions). Using 19 electron micrographs taken from three mice, we analyzed the total number of 13, 11, 56, 22, and 61 synaptic elements. $*P < 0.01$ compared with all other labelings; NS, $P > 0.05$ compared with postsynaptic labeling at inhibitory synapses; $\#P < 0.05$ compared with presynaptic labeling at flat synapses and postsynaptic labeling at axospinous synapses, Mann–Whitney *U* test. (*F*) Parvalbumin (PV) is detected in presynaptic terminals forming flat perisomatic synapses, but not invaginating synapses. Sp, spine; Te, terminal. (Scale bars: 500 µm.)

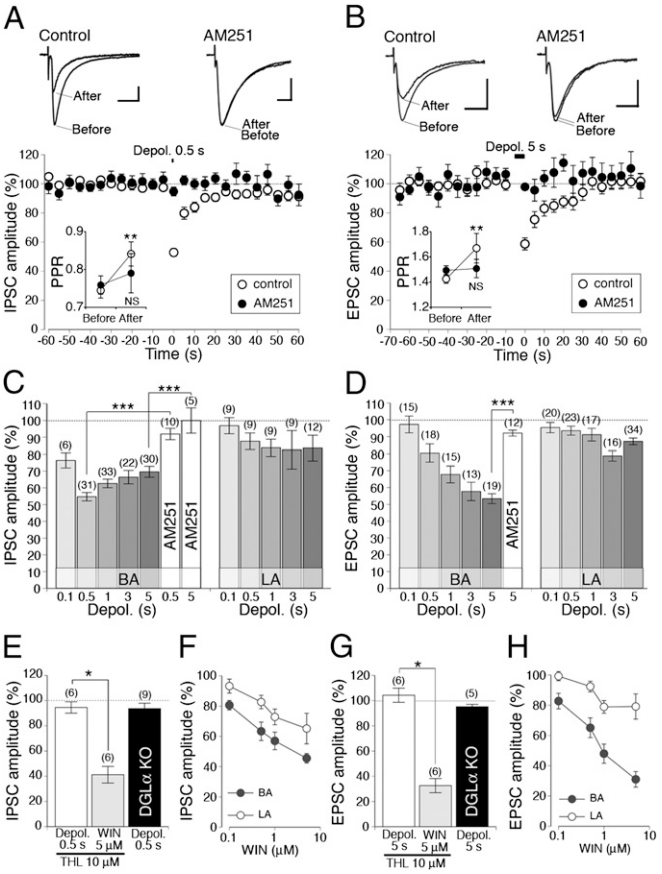

Fig. 5. Induction profiles and properties of DSI (*A, C,* and *E*) and DSE (*B, D,* and *F*) in BA pyramidal neurons and comparison with those in LA pyramidal neurons. (*A* and *B*) Effects of depolarization (from –70 to 0 mV; 0.5 s for DSI and 5 s for DSE) on IPSC/EPSC in BA pyramidal neurons. (*A* and *B Upper*) Example of IPSC/EPSC traces obtained before and after the depolarization. (*A* and *B Lower*) Averaged time course of changes in IPSC/EPSC amplitudes induced by depolarization in the control (open symbols; $n = 35$ for DSI and $n = 19$ for DSE) and after bath-application of 5 µM AM251 (closed symbols; $n = 7$ for DSI and $n = 5$ for DSE). (*C* and *D*) Summary bar graphs for the changes in IPSC/EPSC amplitudes by increasing the duration of depolarizing stimuli in BA (*Left*) or LA (*Right*) pyramidal neurons. Numbers of tested cells are indicated in the parentheses. $***P < 0.001$, Mann–Whitney *U* test. (*E* and *G*) Average IPSC/EPSC amplitudes induced by depolarization in the presence of 10 µM THL before (*Left*) and after (*Center*) bath application of 5 µM WIN, or by depolarization in DGLα-knockout mice (*Right*). Numbers of tested samples are indicated in the parentheses. (*F* and *H*) Dose-dependent decreasing of IPSC/EPSC amplitudes by bath application of WIN in BA (filled circles) and LA (open circles) pyramidal neurons (IPSC: BA, $n = 5$, LA, $n = 5$; EPSC: BA, $n = 9$, LA, $n = 9$). $*P < 0.05$, Wilcoxon signed-rank test. Calibration: 100 pA, 10 ms.

duced no change in IPSC amplitudes ($101.9 \pm 2.0\%$, $n = 5$). Thus, DSI and DSE were caused by CB_1-mediated suppression of presynaptic release of GABA and glutamate, respectively.

When changing the duration of depolarizing pulse from 0.1 s to 5 s, DSI was induced even by the shortest depolarization of 0.1 s and reached the maximal suppression at the depolarization of 0.5 s (Fig. 5*C, Left*), suggesting that DSI was saturated already at 0.5 s. In contrast, DSE was not observed by depolarizing pulse of 0.1 s and induced with progressively larger magnitudes by depolarization from 0.5 s to 5 s (Fig. 5*D, Left*). Both DSI and DSE were mediated by 2-AG produced by DGLα, because they were completely blocked by application of 10 µM DGL inhibitor THL (depolization 0.5 s for IPSC, $94.5 \pm 4.4\%$, $n = 6$; depolization 5 s for EPSC, $104.2 \pm 5.6\%$, $n = 6$), and were absent in DGLα-knockout mice (depolization 0.5 s for IPSC, $93.6 \pm 4.1\%$, $n = 9$; depolization 5 s for EPSC, $95.1 \pm 1.8\%$, $n = 6$) in BA pyramidal neurons (Fig. 5 *E* and *G*). Even in the presence of THL, application of cannabinoid receptor agonist WIN (5 µM) could suppress IPSC ($41.1 \pm 6.6\%$, $n = 6$) and EPSC ($32.6 \pm 7.1\%$, $n = 5$) (Fig. 5 *E* and *G*), indicating that THL did not influence CB_1 receptor sensitivities of presynaptic terminals. Therefore, DGLα is indispensable for DSI and DSE in BA pyramidal neurons with DSI being more easily induced and saturated than DSE.

Compared with BA pyramidal neurons, DSI and DSE in LA pyramidal neurons were apparently low in magnitude and high in induction threshold (Fig. 5 *C* and *D, Right*). Decay time constant of recovery for DSI induced by 0.5-s depolarization was shorter in the BA (5.7 s) than in the LA (6.5 s), whereas that for DSE induced by 5-s depolarization was comparable in both nuclei (8.3 s for each). We then applied different concentrations of WIN to compare the magnitude of suppression. At all WIN concentrations, amplitudes of both IPSC and EPSC were reduced to larger extents in the BA than in the LA (Fig. 5 *F* and *H*), indicating higher CB_1 sensitivities in BA pyramidal neurons.

Invaginating Synapse Enriched with 2-AG Signaling Molecules Is Unique to BA Pyramidal Neuron. All of the results presented so far, together with high CB_1 levels in the BA compared with other amygdala nuclei (Fig. 6*A* and Fig. S3*B*), suggest that BA pyramidal neurons are prone to undergo 2-AG-mediated retrograde

suppression. Finally, we compared the molecular-structural configuration in BA pyramidal neurons with that in LA pyramidal neurons. Average fluorescence intensity for CB_1 (Fig. 6 *B–D*) or MGL (Fig. 6 *B*, *C*, and *E*) in CB_1-positive/VIAAT-positive inhibitory terminals was significantly higher in the BA than in the LA. Around VGluT1-positive excitatory terminals in the neuropil (Fig. 6 *F* and *G*), average intensity for CB_1, although much lower than in inhibitory terminals, was significantly higher in the BA than in the LA (Fig. 6*H*). In LA pyramidal neurons, all of the CB_1-positive perisomatic terminals examined (17 synapses) made flat-type synapses (Fig. 6*I*). It has been reported that invaginating synapses are formed between CCK-positive interneurons and granule cells in the dentate gyrus (30, 31). However, we found no specific accumulation of DGLα to invaginating synapses in the dentate gyrus (Fig. S8). Taken altogether, intensive accumulation of 2-AG signaling molecules to pre- and postsynaptic sites of invaginating synapses is unique to BA pyramidal neurons.

Discussion

In this study, we found in the BA a unique type of perisomatic synapses termed here invaginating synapse (Fig. S9, *Left*). At invaginating synapses, the presynaptic element was CCK-positive interneuron terminals expressing high levels of CB_1 and MGL, whereas the postsynaptic element was the somatic membrane of BA pyramidal neurons recruiting high levels of DGLα. By comparison, flat perisomatic synapses formed by parvalbumin-positive interneurons were negative in CB_1 expression and low in MGL expression and exhibited no particular accumulation of DGLα (Fig. S9, *Center*). As a result, almost all perisomatic DGLα clusters were paired with presynaptic terminals coexpressing CB_1 and MGL. Therefore, invaginating synapses in BA pyramidal neurons are distinguished from flat perisomatic synapses by intensive molecular convergence for 2-AG–mediated retrograde signaling. This molecular convergence suggests that GABA release at invaginating synapses is suppressed effectively by 2-AG, which is evidenced by the readiness of induction and saturation of DSI compared with DSE in the BA.

BLA pyramidal neurons are known to induce long-lasing DSI (19, 28) and CB_1-mediated long-term depression (20) at inhibitory synapses, and also induce DSE at excitatory synapses (29). There is accumulating evidence that local inhibitory circuits in the BLA contribute to, or even mediate, fear conditioning and extinction. This function is thought to be executed through modulation of inhibitory gating of long-term potentiation at synapses with sensory inputs to the BLA, generation of theta and gamma oscillations in the BLA, and regulation of BLA outputs to the major output nuclei of the amygdala, i.e., the central medial nucleus and bed nucleus of the stria terminalis (16, 17, 32, 33). Furthermore, CCK-positive interneurons have been proposed to function as fine-tuning devices for the cooperation of principal neurons, which are sensitive to the emotional, motivational, and physiological state of the animal (34). Such modulatory inhibitory inputs from CCK-positive interneurons to BA pyramidal neurons are likely to be the primary target of 2-AG-mediated retrograde modulation. Shut off of the perisomatic inhibition will increase the excitability of BA pyramidal neurons that, in turn, influences and modulates fear conditioning and extinction through direct glutamatergic projection to the major output nuclei and also through indirect disynaptic routes via GABAergic intercalated cell masses and central lateral nucleus (35).

CB_1 and DGLα were also distributed in the neuropil and localized at axospinous synapses of BA pyramidal neurons (Fig. S9, *Right*). Although immunogold labeling at these synapses was several times lower compared with invaginating synapses, BA pyramidal neurons richly express $G_{q/11}$-coupled receptors, such as the muscarinic acetylcholine receptor M_1 (Fig. S10 *A* and *B*) and the metabotropic glutamate receptor $mGluR_5$ (Fig. S10 *D* and *E*). Moreover, DGLα clusters in the neuropil were closely positioned to M_1- and $mGluR_5$-positive clusters (Fig. S10 *C* and *F*). Considering that the BA receives dense innervation by cholinergic, serotonergic, and glutamatergic afferents (36–38), retrograde suppression of glutamate release will be potently influenced by neural activities, neuromodulators, and the state of the brain, which may then affect synaptic integration and plasticity at local dendrites and spines.

In fear conditioning, the LA is involved in unimodal or elemental representations, such as auditory-unconditioned stimulus association, whereas the BA is in contextual representations by integrating polymodal inputs from the hippocampal formation, prefrontal cortex, and perirhinal cortex (39). Magnitudes of DSI and DSE were apparently smaller in the LA than in the BA, and LA pyramidal neurons showed no such invaginating synaptic structure or intensive molecular convergence as BA neurons did. This contrasting configuration between the two major nuclei of the BLA suggests that 2-AG–mediated retrograde suppression plays an important role in processing and integration of polymodal information in the BA.

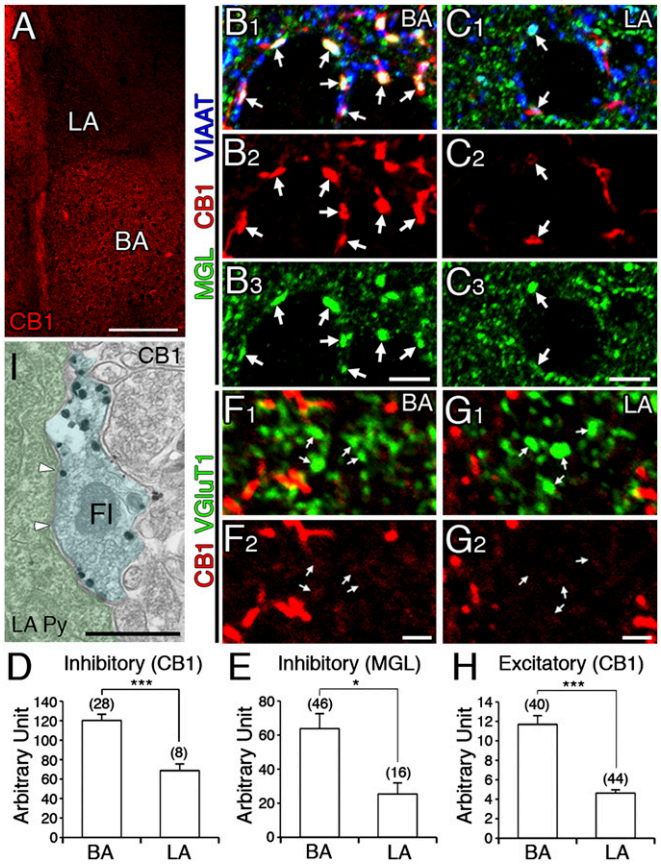

Fig. 6. Distinct molecular expression and synaptic configuration between BA and LA pyramidal neurons. (*A*) Single CB_1 immunofluorescence in the basal (BA) and lateral (LA) nuclei of the basolateral amygdala. Note apparently higher CB_1 intensity in the BA than in the LA. (*B* and *C*) Triple immunofluorescence showing higher intensities of CB_1 and MGL at CB_1-expressing/VIAAT-positive inhibitory terminals (arrows) in the BA than in the LA. (*F* and *G*) Double immunofluorescence showing higher intensities of CB_1 around CB_1-expressing/VGluT1-positive excitatory terminals in the BA than in the LA. (*D, E,* and *H*) Average fluorescence intensities for CB_1 (*D*) and MGL (*E*) at CB_1-expressing/VIAAT-positive inhibitory terminals and for CB_1 around CB_1-expressing/VGluT1-positive excitatory terminals in the BA and LA. Numbers of analyzed terminals are indicated in the parentheses. $*P < 0.05$, $***P < 0.001$, Mann–Whitney *U* test. (*I*) CB_1-expressing perisomatic terminals form flat-type synapse in LA pyramidal neuron. (Scale bars: *A*, 200 μm; *B* and *C*, 5 μm; *F* and *G*, 2 μm; *I*, 500 nm.)

Materials and Methods

Animal. We used adult C57BL/6 mice, CB_1-knockout mice (40), and DGLα-knockout mice (41) in the present study. Breeding pairs of CB_1-knockout mice were kindly provided by A. Zimmer (University of Bonn, Germany). All experiments were

performed according to the guidelines laid down by the animal welfare committees of Hokkaido University. Under deep pentobarbital anesthesia (100 mg/kg of body weight, i.p.), mice were fixed transcardially with 4% paraformaldehyde in 0.1 M sodium phosphate buffer (PB, pH 7.2) for light microscopic histochemistry, 4% paraformaldehyde/0.1% glutaraldehyde in PB for immunoelectron microscopy, and 2% paraformaldehyde-2% glutaraldehyde in PB for conventional electron microscopy.

Anatomy. Procedures of FISH were as reported (42) (*SI Materials and Methods*). The specificity of FISH was confirmed by blank labeling with use of control sense cRNA probes. For immunofluorescence, microslicer sections were incubated successively with 10% normal donkey serum for 30 min, a mixture of primary antibodies overnight (1 μg/mL for each; *SI Materials and Methods*), and a mixture of Alexa 488-, indocarbocyanine (Cy3)-, and indodicarbocyanine (Cy5)-labeled species-specific secondary antibodies for 2 h at a dilution of 1:200 (Invitrogen and Jackson ImmunoResearch). Fluorescent images were taken with a confocal laser-scanning microscope (FV1000; Olympus).

Preembedding immunogold electron microscopy was conducted as reported (42). The number of membrane-attached metal particles divided by the total length of membranes was measured in each pre- and postsynaptic compartment. Inhibitory or excitatory terminals were morphologically identified by the symmetrical or asymmetrical contact, respectively, that they made. Conventional electron microscopy using serial ultrathin sections was done to obtain 3D reconstructed images (*SI Materials and Methods*).

Electrophysiology. Acute slices containing the amygdala were prepared by following our standard procedures for cutting striatal slices (43, 44). Whole-cell voltage-clamp recordings were obtained from BA and LA pyramidal neurons by following our standard procedures for recording from neurons in the striatum (43, 44) and cerebellum (24). These procedures are described in greater detail in *SI Materials and Methods*.

ACKNOWLEDGMENTS. We thank the Center for Ulcer Research and Education Gastroenteric Biology Center at the University of California, Los Angeles for the CCK antibody. This work has been supported in part by the Strategic Research Program for Brain Sciences (Development of Biomarker Candidates for Social Behavior), Grants-in-Aid for Scientific Research 21220006 (to M.K.) and 19100005 (to M.W.), and the Global Center of Excellence Program from the Japanese Ministry of Education, Culture, Sports, Science and Technology. M.U. is a recipient of Research Fellowships of the Japan Society for the Promotion of Science for Young Scientists.

1. Kano M, Ohno-Shosaku T, Hashimotodani Y, Uchigashima M, Watanabe M (2009) Endocannabinoid-mediated control of synaptic transmission. *Physiol Rev* 89:309–380.
2. Bisogno T, et al. (2003) Cloning of the first sn1-DAG lipases points to the spatial and temporal regulation of endocannabinoid signaling in the brain. *J Cell Biol* 163:463–468.
3. Karlsson M, Contreras JA, Hellman U, Tornqvist H, Holm C (1997) cDNA cloning, tissue distribution, and identification of the catalytic triad of monoglyceride lipase. Evolutionary relationship to esterases, lysophospholipases, and haloperoxidases. *J Biol Chem* 272:27218–27223.
4. Dinh TP, et al. (2002) Brain monoglyceride lipase participating in endocannabinoid inactivation. *Proc Natl Acad Sci USA* 99:10819–10824.
5. Katona I, Freund TF (2008) Endocannabinoid signaling as a synaptic circuit breaker in neurological disease. *Nat Med* 14:923–930.
6. Kawamura Y, et al. (2006) The CB1 cannabinoid receptor is the major cannabinoid receptor at excitatory presynaptic sites in the hippocampus and cerebellum. *J Neurosci* 26:2991–3001.
7. Yoshida T, et al. (2006) Localization of diacylglycerol lipase-alpha around postsynaptic spine suggests close proximity between production site of an endocannabinoid, 2-arachidonoylglycerol, and presynaptic cannabinoid CB1 receptor. *J Neurosci* 26:4740–4751.
8. Uchigashima M, et al. (2007) Subcellular arrangement of molecules for 2-arachidonoylglycerol-mediated retrograde signaling and its physiological contribution to synaptic modulation in the striatum. *J Neurosci* 27:3663–3676.
9. LeDoux J (2003) The emotional brain, fear, and the amygdala. *Cell Mol Neurobiol* 23: 727–738.
10. Haller J, Varga B, Ledent C, Freund TF (2004) CB1 cannabinoid receptors mediate anxiolytic effects: Convergent genetic and pharmacological evidence with CB1-specific agents. *Behav Pharmacol* 15:299–304.
11. Viveros MP, Marco EM, Llorente R, Lamota L (2007) The role of the hippocampus in mediating emotional responses to nicotine and cannabinoids: A possible neural substrate for functional interactions. *Behav Pharmacol* 18:375–389.
12. Mailleux P, Vanderhaeghen JJ (1992) Distribution of neuronal cannabinoid receptor in the adult rat brain: A comparative receptor binding radioautography and in situ hybridization histochemistry. *Neuroscience* 48:655–668.
13. Matsuda LA, Bonner TI, Lolait SJ (1993) Localization of cannabinoid receptor mRNA in rat brain. *J Comp Neurol* 327:535–550.
14. Marsicano G, Lutz B (1999) Expression of the cannabinoid receptor CB1 in distinct neuronal subpopulations in the adult mouse forebrain. *Eur J Neurosci* 11:4213–4225.
15. Katona I, et al. (2001) Distribution of CB1 cannabinoid receptors in the amygdala and their role in the control of GABAergic transmission. *J Neurosci* 21:9506–9518.
16. Kamprath K, et al. (2011) *Short-Term Adaptation of Conditioned Fear Responses Through Endocannabinoid Signaling in the Central Amygdala Neuropsychopharmacology* 36:652–663.
17. Davis M, Whalen PJ (2001) The amygdala: Vigilance and emotion. *Mol Psychiatry* 6:13–34.
18. McGaugh JL (2004) The amygdala modulates the consolidation of memories of emotionally arousing experiences. *Annu Rev Neurosci* 27:1–28.
19. Zhu PJ, Lovinger DM (2005) Retrograde endocannabinoid signaling in a postsynaptic neuron/synaptic bouton preparation from basolateral amygdala. *J Neurosci* 25:6199–6207.
20. Marsicano G, et al. (2002) The endogenous cannabinoid system controls extinction of aversive memories. *Nature* 418:530–534.
21. Campolongo P, et al. (2009) Endocannabinoids in the rat basolateral amygdala enhance memory consolidation and enable glucocorticoid modulation of memory. *Proc Natl Acad Sci USA* 106:4888–4893.
22. Ganon-Elazar E, Akirav I (2009) Cannabinoid receptor activation in the basolateral amygdala blocks the effects of stress on the conditioning and extinction of inhibitory avoidance. *J Neurosci* 29:11078–11088.
23. Ohno-Shosaku T, Maejima T, Kano M (2001) Endogenous cannabinoids mediate retrograde signals from depolarized postsynaptic neurons to presynaptic terminals. *Neuron* 29:729–738.
24. Yoshida T, et al. (2002) The cannabinoid CB1 receptor mediates retrograde signals for depolarization-induced suppression of inhibition in cerebellar Purkinje cells. *J Neurosci* 22:1690–1697.
25. Kreitzer AC, Regehr WG (2001) Retrograde inhibition of presynaptic calcium influx by endogenous cannabinoids at excitatory synapses onto Purkinje cells. *Neuron* 29:717–727.
26. Wilson RI, Nicoll RA (2001) Endogenous cannabinoids mediate retrograde signalling at hippocampal synapses. *Nature* 410:588–592.
27. Azad SC, et al. (2004) Circuitry for associative plasticity in the amygdala involves endocannabinoid signaling. *J Neurosci* 24:9953–9961.
28. Patel S, Kingsley PJ, Mackie K, Marnett LJ, Winder DG (2009) Repeated homotypic stress elevates 2-arachidonoylglycerol levels and enhances short-term endocannabinoid signaling at inhibitory synapses in basolateral amygdala. *Neuropsychopharmacology* 34:2699–2709.
29. Kodirov SA, et al. (2010) Endogenous cannabinoids trigger the depolarization-induced suppression of excitation in the lateral amygdala. *Learn Mem* 17:43–49.
30. Leranth C, Frotscher M (1986) Synaptic connections of cholecystokinin-immunoreactive neurons and terminals in the rat fascia dentata: A combined light and electron microscopic study. *J Comp Neurol* 254:51–64.
31. Acsády L, Katona I, Martínez-Guijarro FJ, Buzsáki G, Freund TF (2000) Unusual target selectivity of perisomatic inhibitory cells in the hilar region of the rat hippocampus. *J Neurosci* 20:6907–6919.
32. Ehrlich I, et al. (2009) Amygdala inhibitory circuits and the control of fear memory. *Neuron* 62:757–771.
33. Pape HC, Pare D (2010) Plastic synaptic networks of the amygdala for the acquisition, expression, and extinction of conditioned fear. *Physiol Rev* 90:419–463.
34. Freund TF (2003) Interneuron Diversity series: Rhythm and mood in perisomatic inhibition. *Trends Neurosci* 26:489–495.
35. Amano T, Unal CT, Paré D (2010) Synaptic correlates of fear extinction in the amygdala. *Nat Neurosci* 13:489–494.
36. Ben-Ari Y, Zigmond RE, Shute CC, Lewis PR (1977) Regional distribution of choline acetyltransferase and acetylcholinesterase within the amygdaloid complex and stria terminalis system. *Brain Res* 120:435–444.
37. McDonald AJ (1998) Cortical pathways to the mammalian amygdala. *Prog Neurobiol* 55:257–332.
38. Muller JF, Mascagni F, McDonald AJ (2007) Serotonin-immunoreactive axon terminals innervate pyramidal cells and interneurons in the rat basolateral amygdala. *J Comp Neurol* 505:314–335.
39. Onishi BK, Xavier GF (2010) Contextual, but not auditory, fear conditioning is disrupted by neurotoxic selective lesion of the basal nucleus of amygdala in rats. *Neurobiol Learn Mem* 93:165–174.
40. Zimmer A, Zimmer AM, Hohmann AG, Herkenham M, Bonner TI (1999) Increased mortality, hypoactivity, and hypoalgesia in cannabinoid CB1 receptor knockout mice. *Proc Natl Acad Sci USA* 96:5780–5785.
41. Tanimura A, et al. (2010) The endocannabinoid 2-arachidonoylglycerol produced by diacylglycerol lipase alpha mediates retrograde suppression of synaptic transmission. *Neuron* 65:320–327.
42. Yamasaki M, Matsui M, Watanabe M (2010) Preferential localization of muscarinic M1 receptor on dendritic shaft and spine of cortical pyramidal cells and its anatomical evidence for volume transmission. *J Neurosci* 30:4408–4418.
43. Narushima M, et al. (2007) Tonic enhancement of endocannabinoid-mediated retrograde suppression of inhibition by cholinergic interneuron activity in the striatum. *J Neurosci* 27: 496–506.
44. Narushima M, Uchigashima M, Hashimoto K, Watanabe M, Kano M (2006) Depolarization-induced suppression of inhibition mediated by endocannabinoids at synapses from fast-spiking interneurons to medium spiny neurons in the striatum. *Eur J Neurosci* 24: 2246–2252.